GENETICS

Cold acclimation via the KQT-2 potassium channel is modulated by oxygen in *Caenorhabditis elegans*

Misaki Okahata[1], Aguan D. Wei[2], Akane Ohta[1,3,4]*, Atsushi Kuhara[1,3,4,5]*

Adaptive responses to external temperatures are essential for survival in changing environments. We show here that environmental oxygen concentration affects cold acclimation in *Caenorhabditis elegans* and that this response is regulated by a KCNQ-type potassium channel, KQT-2. Depending on culture conditions, *kqt-2* mutants showed supranormal cold acclimation, caused by abnormal thermosensation in ADL chemosensory neurons. ADL neurons are responsive to temperature via transient receptor potential channels—OSM-9, OCR-2, and OCR-1—with OCR-1 negatively regulating ADL function. Similarly, KQT-2 and KQT-3 regulate ADL activity, with KQT-2 positively regulating ADL function. Abnormal cold acclimation and acute temperature responses of ADL neurons in *kqt-2* mutants were suppressed by an oxygen-receptor mutation in URX coelomic sensory neurons, which are electrically connected to ADL via RMG interneurons. Likewise, low oxygen suppressed supranormal *kqt-2* cold acclimation. These data thus demonstrate a simple neuronal circuit integrating two different sensory modalities, temperature and oxygen, that determines cold acclimation.

INTRODUCTION

Physiological responses to sustained temperature changes constitute a critical adaptive mechanism for living organisms, including humans. Most animals sense temperature by specialized thermosensory neurons, which transduce and deliver thermal information to the many organs of the body. Molecular mechanisms for thermosensation in neurons are crucial for responding to temperature change. Although transient receptor potential (TRP) channels are known temperature receptors in many species (*1*), TRP-independent temperature-sensing mechanisms are also present in nematodes and flies (*2, 3*).

In *Drosophila* larvae, choice of optimal temperature is controlled by a nontemperature receptor-type TRP channel, which is activated through G_q signaling containing phospholipase C. In this cascade, rhodopsin is thought to be required for temperature sensation (*2*). Temperature responses of the nematode *Caenorhabditis elegans* have been studied in various phenomena, such as thermotaxis, noxious heat avoidance, and cold tolerance (*4–7*). In thermotaxis, temperature information is mainly received by the AFD sensory neuron via receptor-type guanylyl cyclases (rGCs), phosphodiesterase, and the guanosine 3′,5′-monophosphate (cGMP)–dependent channel, where rGCs are thought to act as a temperature receptor (*3*). In noxious heat avoidance, the TRP channel encoded by the *osm-9* gene acts as a primary channel in the sensation of noxious heat (*8, 9*). The signaling through transient receptor potential vanilloid (TRPV) channels, OSM-9 and OCR-2, control behavioral responses to noxious heat (*10*).

C. elegans has mechanisms to acclimate to environmental temperature changes, for example, by changing lipid composition and rapidly regulating their metabolism and behavior under sustained temperature changes (*7, 11–14*). Previous studies have reported that cold tolerance of *C. elegans* is regulated by a pair of head sensory neurons, ASJ, in which heterotrimeric G proteins and cGMP signaling transduce temperature information into electrical activity (*7, 15*). ASJ neurons release insulin to intestinal cells to control the cold-tolerant status of individual animals (*7*). It has also been reported that sperm affects the activity of ASJ temperature-sensing neurons in cold tolerance (*16*). Recently, the ADL sensory neuron known to be involved in chemosensation was also shown to be responsive to temperature through TRP channels to regulate cold tolerance (*17*).

C. elegans wild-type strains demonstrate a form of acclimation related to cold tolerance, which we define as cold acclimation (*7, 18*). Wild-type N2 animals cultivated at 25°C do not survive at 2°C, whereas wild-type animals cultivated at 15°C survive at 2°C. However, when wild-type animals cultivated at 25°C are transferred to 15°C and maintained at 15°C for 3 hours, they become capable of survival at 2°C (*7, 18*). Natural *C. elegans* variants show varying degrees of this cold acclimation phenotype, which correlates with genetic polymorphisms that map to multiple regions of the genome (*18*). The genes involved in cold acclimation have not been determined, and the molecular/physiological mechanisms underlying cold acclimation in *C. elegans* remain poorly understood.

KCNQ-type potassium channels play a wide range of physiological roles in human. Mutations of the KCNQ gene family cause hereditary diseases, including neonatal epilepsy, cardiac arrhythmia, and progressive deafness (*19–24*). The *C. elegans* genome contains three genes encoding KCNQ-like potassium channel subunits: *kqt-1*, *kqt-2*, and *kqt-3*. KQT channels (K^+ channel related to QT interval), KQT-1 and KQT-3, are expressed in chemosensory neurons, mechanosensory neurons, and intestinal cells (*25*). In the intestine, KQT channels have an important role in promoting Ca^{2+} oscillations. *kqt-2* and *kqt-3* are proposed to regulate the defecation cycle through a rhythmic Ca^{2+}/calmodulin-dependent control of the driving force for Ca^{2+} influx into intestinal cells (*26*). In rat, KCNQ channels are expressed in nociceptive cold-sensing trigeminal ganglion neurons and play a role in controlling cold sensitivity (*27*). However, a role for KCNQ-type potassium channels in the organismal control of temperature acclimation in individual animals has not been reported.

[1]Graduate School of Natural Science, Konan University, Kobe 658-8501, Japan. [2]Center for Integrative Brain Research, Seattle Children's Research Institute, 1900 Ninth Ave., Seattle, WA 98101, USA. [3]Institute for Integrative Neurobiology, Konan University, Kobe 658-8501, Japan. [4]Faculty of Science and Engineering, Konan University, Kobe 658-8501, Japan. [5]AMED-PRIME, Japan Agency for Medical Research and Development, Tokyo 100-0004, Japan.
*Corresponding author. Email: atsushi_kuhara@me.com (A.K.); aohta@center.konan-u.ac.jp (A.O.)

C. elegans can sense ambient oxygen, which triggers changes in social aggregation behavior. Oxygen is sensed by the oxygen receptor GCY-35/36 in URX coelomic sensory neurons (*28, 29*), which directly connect to RMG interneurons by reciprocal chemical synapses and gap junctions (*30*). Oxygen signaling by URX neurons modulates other head sensory neurons, including ADL, through RMG interneurons (*30*). High oxygen tension decreases the chemosensitivity of ADL neurons for sensing ascaroside, whereas low oxygen tension increases ADL activity, consistent with oxygen modulating ADL activity indirectly through URX and RMG neurons (*30*).

TRP channels are involved in sensory signaling for sensing touch, hearing, taste, vision, smell, and temperature (*31*). In *C. elegans*, the *osm-9* gene encoding the TRPV channel is expressed in sensory neurons involved in osmotic avoidance and chemotaxis to attractive odorants (*32*). The *osm-9* gene is also expressed in sensory neurons involved in noxious heat avoidance and is a primary channel in the sensation of noxious heat (*8–10*).

ocr-2 and *osm-9* are required to respond to aversive stimuli from food and to promote social feeding behavior via ASH and ADL nociceptive neurons (*33*). A dominant-negative mutation of the *C. elegans* TRPV subunit OCR-2, which incorporates into and inactivates OCR-2 homomeric and heteromeric (OCR-2/OCR-1 and OCR-2/OCR-4) TRPV channels, results in a premature egg-laying defect (*34*). Although our recent study indicates that *ocr-2;osm-9;ocr-1* triple mutants show a defect in cold tolerance and decreased thermosensitivity in ADL neurons (*17*), it did not reveal the individual role of each TRP channel subunit in the control of ADL thermosensitivity.

Here, we report that a *kqt-2* mutant defective in a KQT-type potassium channel exhibits supranormal cold acclimation. This enhanced cold acclimation of the *kqt-2* mutant was rescued by expressing *kqt-2 cDNA* in ADL chemosensory neurons. Ca^{2+} imaging revealed that KQT-2 in ADL neurons acts as a positive regulator to temperature changes. We found that the abnormal cold acclimation of *kqt-2* mutants was affected by oxygen concentration during cultivation. Low oxygen concentration suppressed supranormal cold acclimation of the *kqt-2* mutant. Similarly, supranormal cold acclimation of the *kqt-2* mutant mediated by ADL neurons was suppressed by *gcy-35* mutations that impair the oxygen receptor in the URX sensory neuron that communicates with ADL. Our genetic and Ca^{2+} imaging results reveal that oxygen acts as a modulator of temperature sensation in a small neural circuit controlling cold acclimation.

RESULTS

kqt-2 mutant shows supranormal cold acclimation

Cold tolerance in *C. elegans* depends on cultivation temperature. Wild-type animals cultivated at 25°C do not survive at 2°C. By contrast, wild-type animals cultivated at 15°C survive at 2°C (*7*). Cold tolerance exhibits plasticity, dependent on the temperature and length of time of the previous cultivation environment (*7, 18*). When wild-type animals cultivated at 25°C are transferred to 15°C for some hours, animals survive upon subsequent transfer to 2°C (Fig. 1A). Similarly, when wild-type animals cultivated at 15°C are transferred to 25°C for 3 hours, animals fail to survive upon subsequent transfer to 2°C (*7, 18*).

To isolate new genes involved in temperature acclimation, we used results from a previous DNA microarray analysis (*35*). When animals were transferred to 17°C for 4 hours after cultivation from eggs to adult at 23°C, expression levels of 79 genes were significantly changed compared with controls raised at 23°C (*35*). We investigated temperature acclimation phenotypes in a subset of 14 mutants of these genes (fig. S1, A to F). We tested the cold acclimation phenotype of these mutants by cultivating at 25°C, transferring to 15°C for varying lengths of time, and then testing for survival at 2°C (25°C→15°C→2°C; fig. S1, A to C). When 25°C cultivated animals were transferred and conditioned at 15°C for 0, 3, or 8 hours and then transferred to 2°C, survival rates for wild-type animals were 5, 30, and 44%, respectively (fig. S1, A to C). We found that mutants defective in several genes identified from the previous microarray data, including the KQT-type potassium channel subunit, *kqt-2*, showed abnormal cold acclimation under this 25°C→15°C→2°C protocol (Fig. 1, B to D). Although *kqt-2* mutants showed a normal phenotype when animals cultivated at 25°C were exposed to 2°C without a conditioning temperature shift from 25° to 15°C [25°C→15°C (0 hours)→2°C; Fig. 1B], *kqt-2* mutants exhibited an abnormal increase in survival rate at 2°C after conditioning shifts from 25° to 15°C [25°C→15°C (3 or 8 hours)→2°C; Fig. 1, C and D]. By contrast, *kqt-2* mutants showed normal acclimation in a reverse temperature conditioning protocol [15°C→25°C (0, 3, and 8 hours)→2°C; Fig. 1, E to G].

We previously determined various molecules for temperature sensation in the nervous system that regulate cold tolerance. Most of the molecules we identified involve cGMP-dependent signaling, including guanylyl cyclases and cGMP-gated channels. Although cGMP-gated channels are the primary channels for depolarizing membrane potential in thermosensitive neurons, cGMP-gated channel-independent mechanisms for regulating membrane potential in neurons involved in cold tolerance have not been well characterized. We thus focused on the KQT-2 potassium channel as a novel temperature signaling mechanism.

We confirmed that the cold acclimation abnormality of *kqt-2(ok732)* is caused by mutations in the *kqt-2* gene by two means: by analysis of another mutant allele of *kqt-2* [*kqt-2(tm642)*] and by transgenic rescue of *kqt-2(ok732)* with a wild-type genomic *kqt-2(+)* array. *kqt-2(tm642)* exhibited a supranormal cold acclimation phenotype using the 25°C→15°C (3 hours)→2°C protocol, similar to *kqt-2(ok732)* (Fig. 1H). Both *kqt-2* mutant alleles lack most of the exons encoding the channel pore of KQT-2 (*25*), indicating that both alleles are null alleles. The abnormal cold acclimation of *kqt-2(ok732)* was rescued by transgenic expression of a wild-type *kqt-2* genomic gene construct driven by its native promoter (Fig. 1I). These results indicate that KQT-2 is required for normal cold acclimation.

The potassium channel subunit KQT-2 is expressed in sensory neurons

Previous reports described the KQT-2 potassium channel as only expressed in intestine (*25*); therefore, we hypothesized that enhanced cold acclimation of the *kqt-2* mutant is caused by abnormal intestine function. We thus expressed *kqt-2 cDNA* in the intestine of the *kqt-2(ok732)* mutant, driven by the intestine-specific promoter *ges-1p*. However, the abnormal cold acclimation of *kqt-2(ok732)* was not rescued by expressing *kqt-2 cDNA* in intestine (Fig. 1J). Because previous reports revealed that cold acclimation of *C. elegans* is regulated by sensory neurons, as well as intestine, we then specifically expressed *kqt-2 cDNA* in ciliated sensory neurons in *kqt-2(ok732)* mutant using the *osm-6p* promoter. We found that the abnormally enhanced cold acclimation of *kqt-2(ok732)* was rescued by expressing *kqt-2 cDNA* in ciliated sensory neurons (Fig. 1J). To identify the

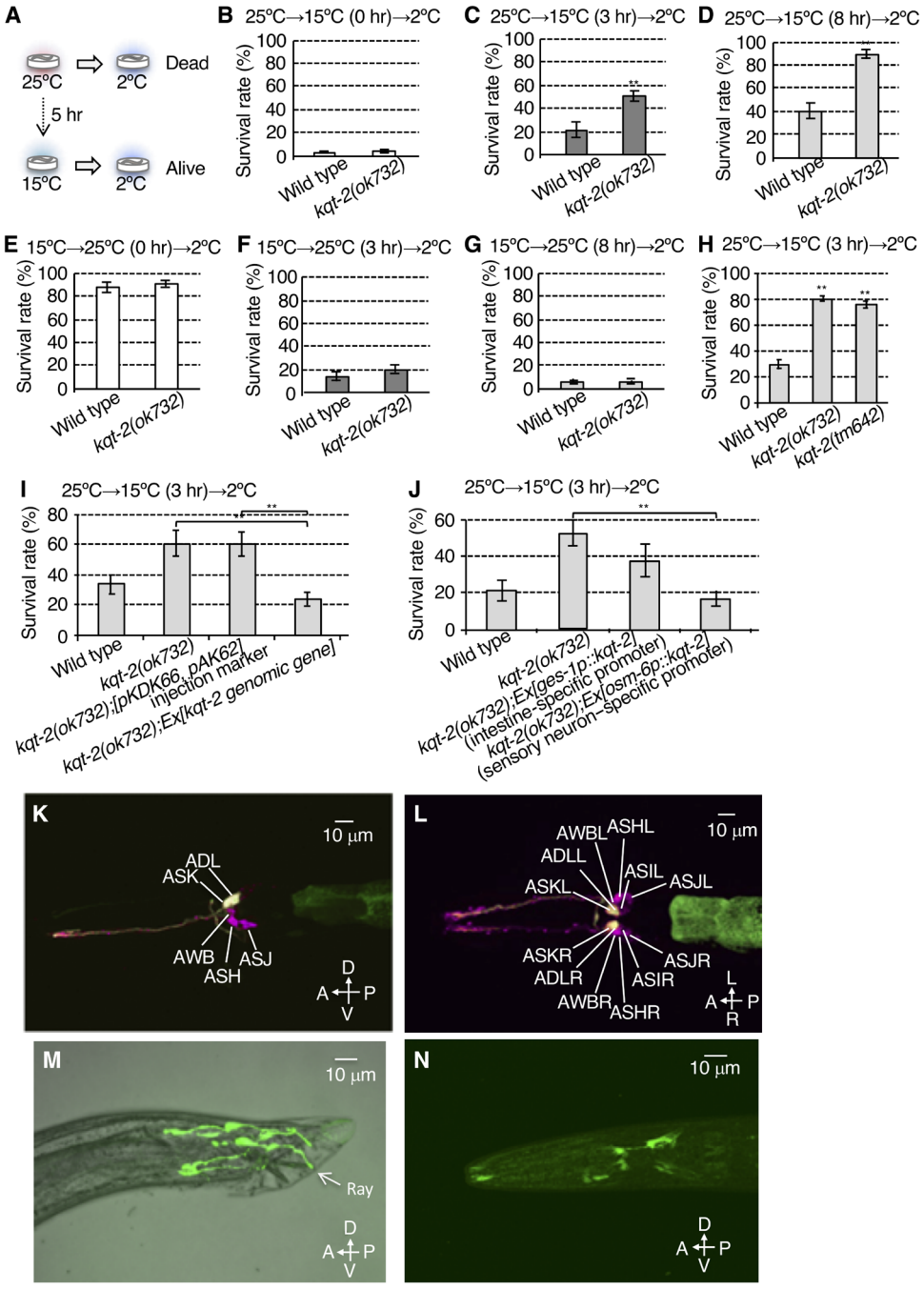

Fig. 1. KQT-2 in sensory neurons regulates cold acclimation. (**A**) Cold acclimation assay. Wild-type animals cultivated at 25°C fail to survive at 2°C, whereas animals cultivated at 15°C survive at 2°C. When wild-type animals cultivated at 25°C are transferred to and conditioned at 15°C for 5 hours, they exhibit increased survival at 2°C. (**B** to **D**) Cold acclimation of *kqt-2(ok732)* mutants assayed by the 25°C→15°C→2°C protocol. *kqt-2(ok732)* exhibited supranormal cold acclimation. Number of assays ≥ 12. (**E** to **G**) Cold acclimation of *kqt-2(ok732)* mutants assayed by the 15°C→25°C→2°C protocol. Number of assays ≥ 10. (B to G) Error bar indicates SEM. Comparisons were performed using the unpaired *t* test (Welch). $^{*}P < 0.05$, $^{**}P < 0.01$. (**H**) Two *kqt-2* loss-of-function mutants exhibited supranormal cold acclimation. Number of assays ≥ 11. Error bar indicates SEM. Comparisons were performed using Dunnett's test. $^{*}P < 0.05$, $^{**}P < 0.01$. (**I**) Transgenic rescue of *kqt-2(ok732)* with a genomic fragment encompassing the wild-type *kqt-2(+)* gene and native promoter sequence. Number of assays ≥ 8. (**J**) Rescue of *kqt-2* mutants by tissue-specific expression of *kqt-2* cDNA. Number of assays ≥ 9. (I and J) Error bar indicates SEM. Comparisons were performed using the Tukey-Kramer method. $^{*}P < 0.05$, $^{**}P < 0.01$. (**K** to **N**) *kqt-2::GFP* driven by the *kqt-2* promoter is expressed in ADL and ASK head sensory neurons. GFP fluorescence of ADL and ASK (yellow) neurons are colabeled with DiI, which labels only six pairs of amphid sensory neurons in the head with red fluorescence (magenta). (K) Lateral view. A, anterior; P, posterior; D, dorsal; V, ventral. (L) Ventral view. L, left; R, right. (M) GFP driven by the *kqt-2* promoter is expressed in fan and ray sensory neurons in the tail of males. (N) Wild-type animal expressing *kqt-2cDNA::gfp* (8 ng/μl) using a 9.0-kb *kqt-2* promoter. KQT-2::GFP is observed in whole sensory neurons and is especially localized to sensory endings and cell bodies of head sensory neurons.

ciliated sensory neuron expressing *kqt-2*, we introduced the *kqt-2* genomic sequence encompassing exons 1 to 12 fused in frame with green fluorescent protein (GFP), driven by the *kqt-2* promoter. GFP fluorescence of KQT-2::GFP in the head was observed in two pairs of sensory neurons (Fig. 1, K and L). However, the expression level of *kqt-2* in sensory neurons was lower than that in intestinal cells. In addition, *kqt-2::GFP* was expressed in male tail neurons with processes that elongate to the tip of the tail (Fig. 1M).

To determine the identity of the sensory neurons expressing *kqt-2* in the head, we colabeled *kqt-2::GFP* animals with DiI, which introduces red fluorescence in only six pairs of amphid sensory neurons in the head (Fig. 1, K and L). Only two pairs of DiI-positive sensory neurons, ADL and ASK, were colabeled with *kqt-2::GFP* (Fig. 1, K and L). The observation of *kqt-2* expression in ADL and ASK neurons is consistent with the results, showing that abnormal cold acclimation in *kqt-2* mutants is rescued by expressing *kqt-2 cDNA* in sensory neurons (Fig. 1J) and that the *kqt-2* mutant showed normal chemotaxis to AWA- and AWC-sensed odorants (fig. S4, A and B).

To visualize the subcellular localization of KQT-2 in sensory neurons, we constructed a *kqt-2cDNA::GFP* fusion gene, driven by the native *kqt-2* promoter sequence. KQT-2::GFP was observed to strongly localize to sensory endings and cell bodies of sensory neurons, although it was observed in the entire cytoplasm of sensory neurons (Fig. 1N and fig. S2A). The number of neurons expressing GFP was increased in this animal, indicating that intronic sequences of the *kqt-2* gene may contain inhibitory elements for expression in some neurons.

Expression of *kqt-2* in ADL sensory neurons is sufficient to rescue supranormal cold acclimation of the *kqt-2* mutant

Abnormally enhanced cold acclimation of the *kqt-2* mutant was rescued by expressing *kqt-2* cDNA (complementary DNA) in ciliated sensory neurons (Fig. 1J). To identify the essential sensory neuron(s) required for enhanced cold acclimation of the *kqt-2* mutant, we repeated *kqt-2* cDNA rescue experiments with single cell type–specific promoters. We expressed *kqt-2* cDNA only in ADL or ASK sensory neurons (Fig. 2A). The abnormally enhanced cold acclimation of the *kqt-2* mutant was rescued by expression of *kqt-2* cDNA in ADL but not ASK sensory neurons (Fig. 2A). Because ADL is known as a chemosensory neuron that receives aversive cues, such as 1-octanol and ascaroside pheromones, we tested avoidance behavior of *kqt-2* mutants against 1-octanol (Fig. 2B). *kqt-2* mutants showed decreased avoidance behavior against high concentrations of 1-octanol compared with wild type (Fig. 2B). These results indicate that KQT-2 in ADL sensory neurons is essential for normal cold acclimation and avoidance behavior.

Our recent study suggested that ADL is responsive to temperature in wild-type animals cultivated at 25°C, as monitored by temperature-dependent changes in intracellular Ca^{2+} (*17*). To investigate whether the thermosensation of ADL depends on cultivated temperature, we introduced the genetically encoded Ca^{2+} indicator, cameleon, to perform Ca^{2+} imaging in response to temperature stimuli. ADL sensory neurons in wild-type animals cultivated at 25°C were responsive to temperature changes, with an increase in intracellular Ca^{2+} signal (9 to 10% ratio) in response to temperature shifts from 17° to 23°C (Fig. 2, C and D). By contrast, thermal responses of ADL in wild-type animals cultivated at 15°C were lower (4 to 5% ratio) than that of animals cultivated at 25°C (Fig. 2, C and D). These results indicate that cultivation temperature influences the responsiveness of ADL neurons.

Upon identical temperature stimulation, the Ca^{2+} response in ADL neurons was blunted in *kqt-2* mutants cultivated at 25°C (2 to 3% ratio) (Fig. 2, E and F), which was rescued by ADL-specific expression of *kqt-2 cDNA* (9 to 10% ratio) (Fig. 2, E and F). However, ADL thermosensation in *kqt-2* mutants cultivated at 15°C showed similar responsiveness compared with wild-type animals (Fig. 2, G and H). These results from Ca^{2+} imaging of *kqt-2* mutants are consistent with the cold acclimation phenotype of *kqt-2* mutants; *kqt-2* mutants cultivated at 25°C showed supranormal cold acclimation and blunted thermal responsiveness, and *kqt-2* mutants cultivated at 15°C showed normal cold acclimation and similar thermal responsiveness compared with wild-type controls (Fig. 1, B to G). Thus, physiological and genetic analyses indicate that KQT-2 potassium channel subunits regulate thermosensation and cold acclimation in ADL neurons when animals are cultivated at 25°C.

Another KQT-type potassium channel subunit, KQT-3, plays an opposite role to that of KQT-2 in cold acclimation

Although activated KCNQ potassium channels are expected to decrease the excitability of neurons, unexpectedly, loss of *kqt-2* function in *kqt-2* mutants decreased temperature-dependent activity in ADL neurons (Fig. 2, E and F). To examine how KQT-2 regulates neural activity of ADL neurons, we measured temperature-dependent Ca^{2+} responses in wild-type animals overexpressing *kqt-2 cDNA* in ADL [*N2;Ex(sre-1p::kqt-2cDNA)*; Fig. 2, E and F]. *kqt-2* overexpression in wild-type ADL neurons induced a hyperactive Ca^{2+} response upon temperature stimuli (Fig. 2, I and J), indicating that KQT-2 potassium channel subunits act as a positive regulator of neuronal activity in wild-type ADL. Mammalian KCNQ2 co-assembles with KCNQ3 (*36*). We therefore hypothesized that KQT-2 and other KQT-type potassium channel subunits might coassemble to form heteromeric channels, and that KQT-2 acts as an inhibitor of other KQT subunits.

C. elegans has three KQT-type potassium channels encoded by *kqt-1*, *kqt-2*, and *kqt-3* genes. *kqt-3* is expressed in some sensory neurons including ADL (*25*). To investigate whether *kqt-3* is involved in ADL neurons in response to temperature changes, we performed Ca^{2+} imaging. The Ca^{2+} responses in ADL neurons upon temperature stimuli were strongly augmented in *kqt-3* mutants (15 to 16% ratio) relative to wild-type animals (Fig. 2, K and L).

To examine genetic epistasis between *kqt-2* and *kqt-3* mutations, we constructed a *kqt-2;kqt-3* double mutant and performed Ca^{2+} imaging and cold acclimation tests. Decreased thermal responsiveness of ADL neurons in the *kqt-2* mutant was suppressed by the *kqt-3* mutation, with the *kqt-2;kqt-3* double mutant exhibiting an enhanced thermosensitive Ca^{2+} response (13 to 14% ratio) similar to *kqt-3(aw1)* (Fig. 2, K and L). In addition, the supranormal cold acclimation of the *kqt-2* mutant was also suppressed by the *kqt-3* mutation in the *kqt-2;kqt-3* double mutant (Fig. 2M). These genetic analyses indicate that *kqt-3* is epistatic to *kqt-2*, which is consistent with the hypothesis that KQT-2 negatively regulates KQT-3. Thus, KQT-2 could function as a negative regulator of KQT channel function with respect to thermosensitivity in ADL sensory neurons.

OCR-1, a TRP subunit, acts as a negative regulator of thermosensitive activity in ADL sensory neurons

The KQT-2 potassium channel acts as a positive regulator of thermosensation in ADL neurons for cold acclimation. We next investigated the relationship between KQT-2 and the known temperature signaling pathway in ADL neurons by genetic epistasis analysis. As recently

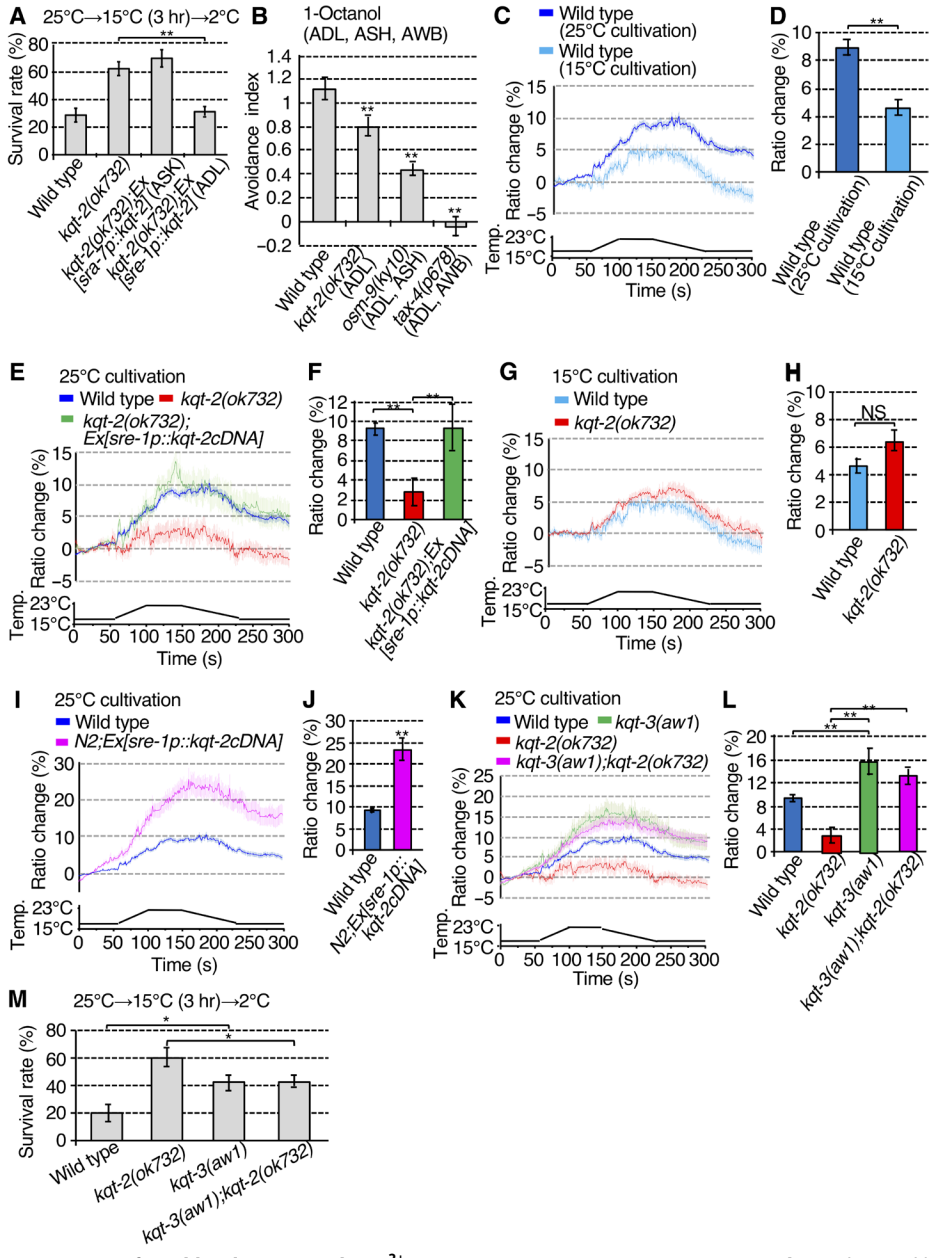

Fig. 2. KQT-2 in ADL neurons is necessary for cold acclimation and a Ca^{2+} response in response to temperature stimuli. (**A**) Abnormal *kqt-2(ok732)* cold acclimation was rescued by expressing *kqt-2*cDNA in ADL, not ASK neurons. Number of assays ≥ 18. Error bar indicates SEM. Comparisons were performed using the Tukey-Kramer method. **P* < 0.05, ***P* < 0.01. (**B**) Avoidance behavior against 1-octanol received by ADL, AWB, and ASH sensory neurons. Number of assays ≥ 9. Error bar indicates SEM. Comparisons were performed using Dunnett's test. **P* < 0.05, ***P* < 0.01. (**C** to **L**) Ca^{2+} imaging of ADL neurons in animals cultivated at 15° or 25°C in response to temperature stimuli from 17° to 23°C. The graphs indicate the change in yellow fluorescent protein (YFP)/cyan fluorescent protein (CFP) ratio in response to temperature stimuli. The bar graphs indicate the average change in ratio from 160 to 170 s (D and H) or from 170 to 180 s (F, J, and L). (C and D) In vivo calcium imaging of ADL neurons in the wild type cultivated at 25° or 15°C. *n* ≥ 16. (E and F) The responsiveness of ADL neurons to temperature change is abrogated in the *kqt-2* mutant and restored by ADL-specific expression of *kqt-2*(+). *n* ≥ 18. (G and H) In vivo calcium imaging of ADL neurons in the wild type and *kqt-2* mutant cultivated at 15°C. *n* ≥ 16. (I and J) Overexpression of *kqt-2(+)* in wild-type ADL neurons increases Ca^{2+} response to temperature stimuli. *n* ≥ 25. (K and L) Increased Ca^{2+} response in ADL neurons in *kqt-3(aw1)* and *kqt-3(aw1);kqt-2(ok732)* mutants. *n* ≥ 16. (D, H, and J) Error bar indicates SEM. Comparisons were performed using the unpaired *t* test (Welch). **P* < 0.05, ***P* < 0.01. (F and L) Error bar indicates SEM. Comparisons were performed using the Tukey-Kramer method. **P* < 0.05, ***P* < 0.01 NS, not significant. Analysis by two-way analysis of variance (ANOVA) confirmed that there was a significant effect of the *kqt-2* genotype (*P* = 0.042) and also a significant effect of the *kqt-3* genotype ($P = 2.20 \times 10^{-8}$), but there was no significant interaction between *kqt-2* and *kqt-3* genotypes (*P* = 0.133; see Supplementary raw data file). Data of wild-type animals cultivated at 25°C, shown in (C), are shared with (E), (I), and (K), Figs. 3 (D, F, and H) and 4D, and fig. S6A, given that the experiments were conducted simultaneously (C, E, I, and K). Data of wild-type animals cultivated at 15°C, shown in (C), are shared with (G), given that the experiments were conducted simultaneously (C and G). Data of *kqt-2(ok723)* cultivated at 25°C, shown in (E), were shared with (K) and Figs. 3H and 4D, given that the experiments were conducted simultaneously (E and K). (**M**) Epistasis analyses of cold acclimation in *kqt-2* and *kqt-3* mutants. All mutant strains exhibit supranormal cold acclimation, but the *kqt-3(aw1)* cold acclimation phenotype appears epistatic to *kqt-2(ok732)*. Number of assays ≥ 12. Error bar indicates SEM. Comparisons were performed using the Tukey-Kramer method. **P* < 0.05, ***P* < 0.01.

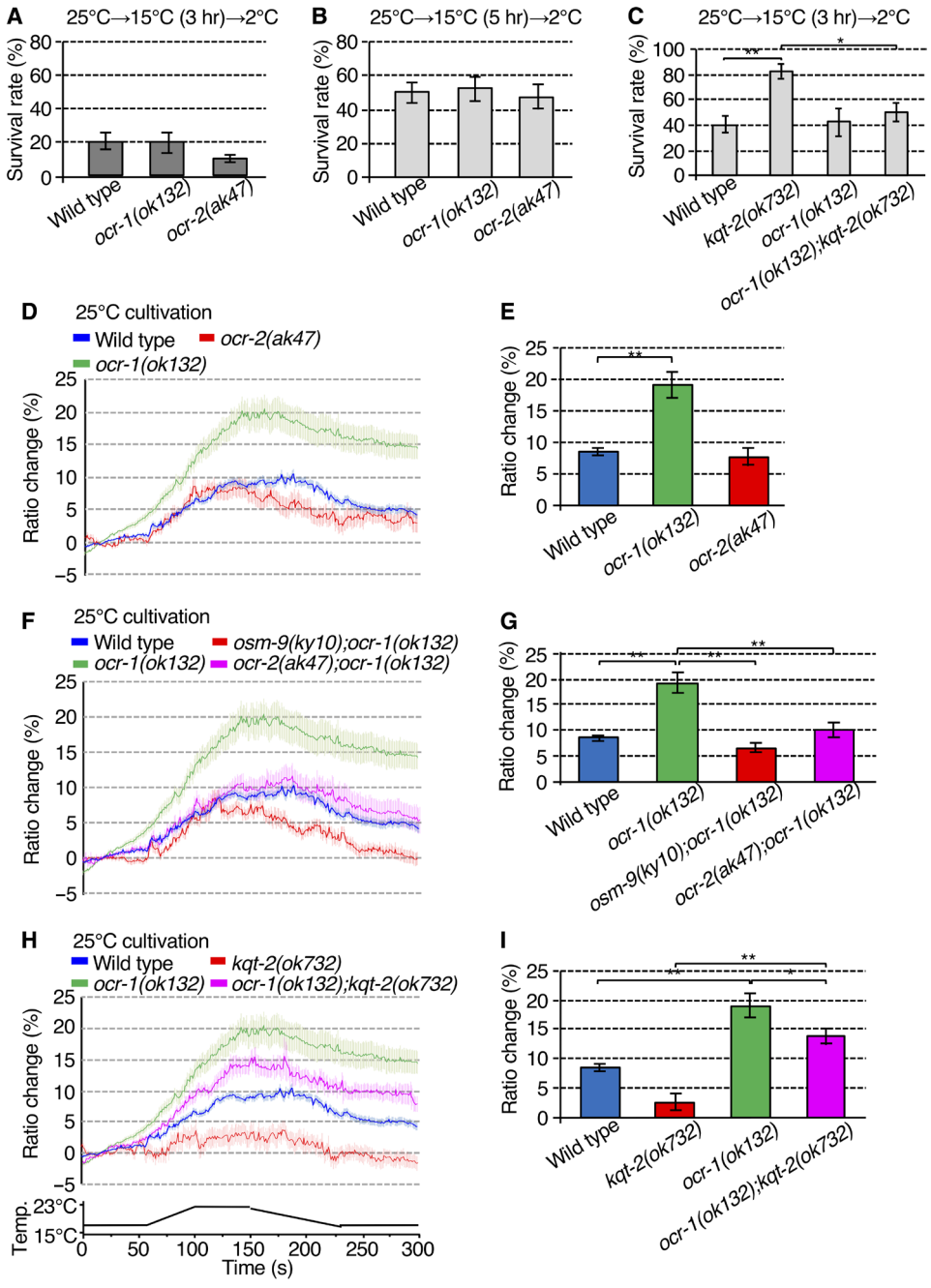

Fig. 3. OCR-1 is a negative regulator of the thermal response in ADL sensory neurons. (**A** and **B**) *ocr-1(ok132)* and *ocr-2(ak47)* mutants did not show abnormal cold acclimation. Number of assays ≥ 13. Error bar indicates SEM. Comparisons were performed using Dunnett's test. (**C**) Supranormal cold acclimation of *kqt-2(ok732)* was suppressed by *ocr-1(ok132)*. Number of assays ≥ 8. Error bar indicates SEM. Comparisons were performed using the Tukey-Kramer method. **P* < 0.05, ***P* < 0.01. (**D** to **I**) Ca^{2+} imaging of ADL neurons in animals cultivated at 25°C in response to a defined temperature ramp. The graph indicates YFP/CFP ratio change in response to temperature stimuli. The bar graph indicates the average ratio change from 140 to 150 s (E, G, and I). (D and E) *ocr-1(ok132)* increases the Ca^{2+} response to temperature stimuli. $n \geq 17$. (F and G) Increased Ca^{2+} thermal response of ADL neurons in *ocr-1(ok132)* is suppressed by *ocr-2(ak47)* or *osm-9(ky10)* mutations. $n \geq 18$. The Ca^{2+} thermal responses in *ocr-2(ak47)* and *osm-9(ky10)* single mutants are described in fig. S6. (H and I) Abrogation of thermal response by *kqt-2(ok732)* loss of function is suppressed in *ocr-1(ok132);kqt-2(ok732)* double mutants. $n \geq 18$. (E) Error bar indicates SEM. Comparisons were performed using Dunnett's test. **P* < 0.05, ***P* < 0.01. (G and I) Error bar indicates SEM. Comparisons were performed using the Tukey-Kramer method. **P* < 0.05, ***P* < 0.01. Wild-type data in (D) are shared with (F) and (H), Figs. 2 (C, E, I, and K) and 4D, and fig. S6A, given that the experiments were conducted simultaneously (D, F, and H). *kqt-2(ok723)* data in (H) are shared with Figs. 2 (E and K) and 4D, given that the experiments were conducted simultaneously. *ocr-1* data in (D) are shared with (F) and (H), given that the experiments were conducted simultaneously (D, F, and H).

reported, temperature signaling in ADL neurons is transmitted through three TRP channel subunits—OSM-9, OCR-1, and OCR-2—to regulate cold tolerance (*17*, *32*, *33*). The *osm-9* mutant and the *ocr-2 osm-9;ocr-1* triple mutant show abnormal cold tolerance (*17*); however, *ocr-1* and *ocr-2* single mutants do not show significantly different cold tolerances compared with the wild type (*17*). We therefore

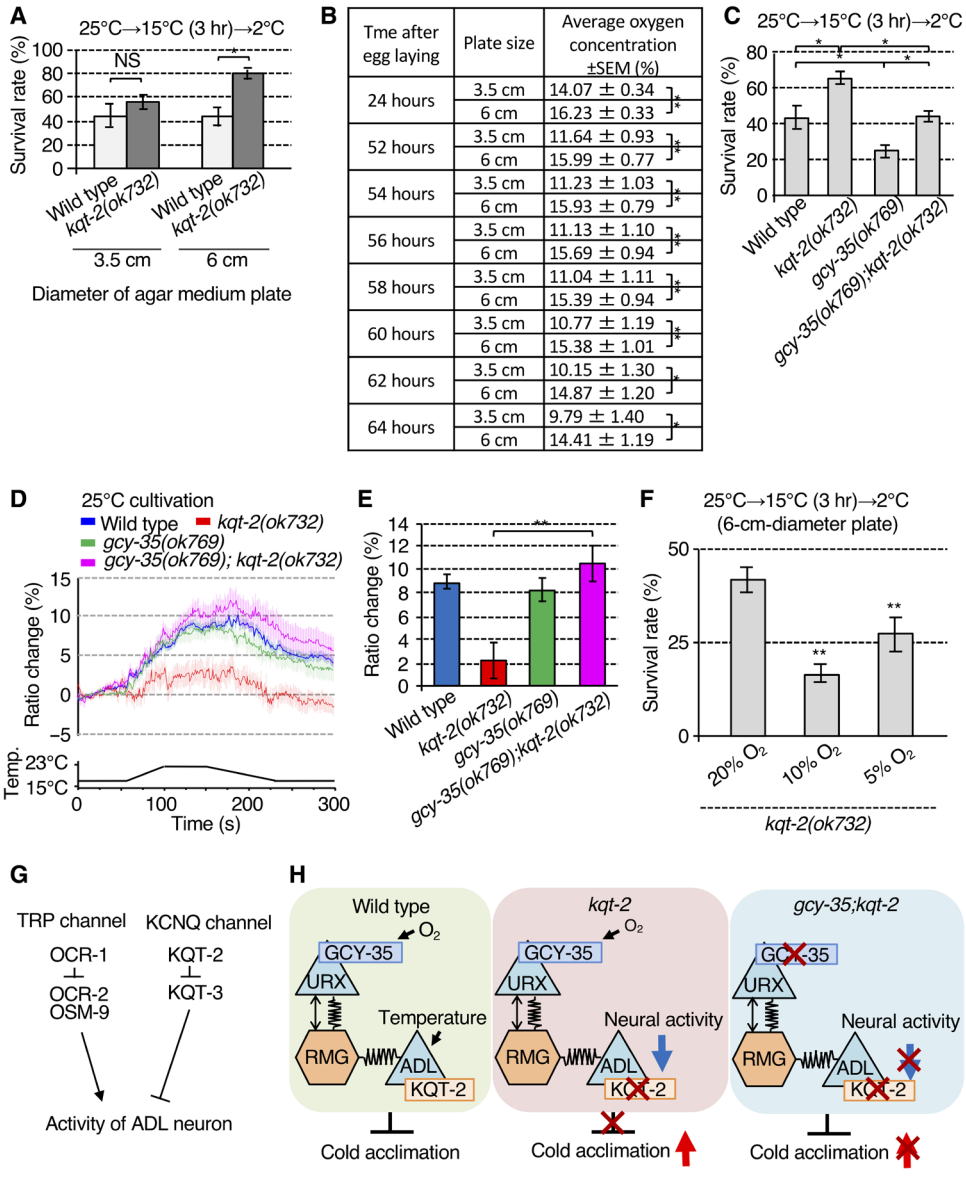

Tme after egg laying	Plate size	Average oxygen concentration ±SEM (%)	
24 hours	3.5 cm	14.07 ± 0.34	**
	6 cm	16.23 ± 0.33	
52 hours	3.5 cm	11.64 ± 0.93	**
	6 cm	15.99 ± 0.77	
54 hours	3.5 cm	11.23 ± 1.03	**
	6 cm	15.93 ± 0.79	
56 hours	3.5 cm	11.13 ± 1.10	**
	6 cm	15.69 ± 0.94	
58 hours	3.5 cm	11.04 ± 1.11	**
	6 cm	15.39 ± 0.94	
60 hours	3.5 cm	10.77 ± 1.19	**
	6 cm	15.38 ± 1.01	
62 hours	3.5 cm	10.15 ± 1.30	*
	6 cm	14.87 ± 1.20	
64 hours	3.5 cm	9.79 ± 1.40	*
	6 cm	14.41 ± 1.19	

Fig. 4. Oxygen signaling modulates ADL-mediated cold acclimation and thermal responsiveness. (**A**) Cold acclimation of animals cultivated on 3.5- and 6.0-cm-diameter plates. Number of assays ≥ 8. Error bar indicates SEM. Comparisons were performed using the Tukey-Kramer method. *P < 0.05, **P < 0.01. (**B**) Oxygen concentration at the surface of 3.5- and 6.0-cm-diameter agar plates with bacterial lawns and worms cultured from 24 to 64 hours after egg laying. Larger 6.0-cm-diameter plates exhibit higher sustained O_2 concentrations. For each point, n = 10. Error bar indicates SEM. Comparisons were performed using the unpaired t test (Welch). *P < 0.05, **P < 0.01. (**C**) *gcy-35* mutant, lacking the intracellular O_2 sensor, suppresses the supranormal cold acclimation of *kqt-2(ok732)*. Number of assays ≥ 11. Error bar indicates SEM. Comparisons were performed using the Tukey-Kramer method. *P < 0.05, **P < 0.01. (**D** and **E**) Abrogation of Ca^{2+} thermal response in ADL neurons of *kqt-2(ok732)* is suppressed in *kqt-2(ok732);gcy-35(ok769)*. n ≥ 18. Error bar indicates SEM. Comparisons were performed using the Tukey-Kramer method. *P < 0.05, **P < 0.01. The bar graph indicates the average ratio change from 160 to 170 s (E). Wild-type data in (D) are shared with Figs. 2 (C, E, I, and K) and 3 (D, F, and H) and fig. S6A, given that the experiments were conducted simultaneously (D). *kqt-2(ok723)* data in (D) are shared with Figs. 2 (E and K) and 3H, given that the experiments were conducted simultaneously (D). (**F**) Enhanced cold acclimation of *kqt-2* was recovered to a normal level after cultivation under 5% O_2. Number of assays ≥ 9. Error bar indicates means SEM. Comparisons were performed using Dunnett's test. *P < 0.05, **P < 0.01. (**G**) Model of molecular mechanisms regulating activity in ADL neurons. OCR-1 acts as a negative regulator of OCR-2/OSM-9 thermally responsive TRP channels in ADL neurons. KQT-2 acts as a negative regulator of KQT-3 potassium channels. (**H**) Model of neuronal circuitry integrating ADL temperature sensing with oxygen signaling by URX visceral oxygen sensory neurons via RMG hub interneurons. In wild-type worms, URX neurons may indirectly modulate temperature signaling of ADL neurons in cold acclimation. Left: Sensing of high O_2 levels by URX neurons, which is dependent on GCY-35, is signaled through RMG to ADL neurons via chemical and electrical synapses to promote cold acclimation, presumably by inhibiting ADL excitability. Middle: Loss of KQT-2 in ADL neurons results in decreased neuronal activity in response to temperature change and increased cold acclimation. Loss of GCY-35 blocks active O_2 signaling from URX neurons, mimicking a low O_2 environment. This increases ADL excitability sufficiently to suppress the inhibitory effect of KQT-2 loss of function. Right: Supranormal cold acclimation observed in *kqt-2* mutants is thus suppressed by *gcy-35* mutations or low O_2 concentration.

performed cold acclimation assays and Ca^{2+} imaging of ADL neurons in *ocr-1* and *ocr-2* mutant backgrounds. Each *ocr-1* and *ocr-2* single mutant showed no significant abnormality in cold acclimation (Fig. 3, A and B). However, supranormal cold acclimation of the *kqt-2* mutant was suppressed by *ocr-1* mutation, indicating that the *ocr-1* mutation is epistatic to the *kqt-2* mutation in cold acclimation (Fig. 3C).

The thermally induced Ca^{2+} response of ADL neurons in the *ocr-1* mutant (19 to 20% ratio) was significantly increased compared with the wild type (8 to 9% ratio; Fig. 3, D and E). This result was unexpected because TRP channels are known as nonspecific cation channels whose activation induces depolarization-promoted Ca^{2+} influx, whereas loss of function of TRP channels decreases neuronal excitability. The increased thermally induced Ca^{2+} response of ADL neurons in *ocr-1* mutants was suppressed by *osm-9* and *ocr-2* mutations in *osm-9;ocr-1* and *ocr-2;ocr-1* double mutants (Fig. 3, F and G, and fig. S6, A and B), indicating that *osm-9* and *ocr-2* mutations are epistatic to *ocr-1* mutation (Fig. 4G). We found that hyperactivation of the ADL thermally induced Ca^{2+} response in *ocr-1* mutants was partially suppressed by *kqt-2* mutation in *ocr-1;kqt-2* double mutants [*ocr-1(ok132);kqt-2(ok732);* Fig. 3, H and I], and the *ocr-1;kqt-2* double mutant showed an intermediate phenotype between respective *ocr-1* and *kqt-2* single mutants by Ca^{2+} imaging [*ocr-1(ok132); kqt-2(ok732)*; Fig. 3, H and I]. This genetic epistasis indicates that the OCR-1 TRP channel–mediated mechanism acts in parallel with KQT-2 potassium channels in the regulation of ADL neural activity for thermosensation (Fig. 4G). Together, epistasis analyses using cold acclimation and ADL thermally induced Ca^{2+} responses indicate that OCR-1 and KQT-2 act in the same genetic pathway for cold acclimation, while OCR-1 functions in parallel with KQT-2 in the thermosensitive Ca^{2+} response in ADL neurons.

Oxygen sensing modulates ADL-mediated cold acclimation

We unexpectedly found that the abnormal cold acclimation of the *kqt-2* mutant was exaggerated when *kqt-2* mutants were cultivated on medium-size (6.0-cm-diameter) agar plates compared with smaller (3.5-cm-diameter) plates (Fig. 4A). Animals cultivated from egg to adult on 3.5-cm-diameter plates did not show a significant difference in cold acclimation compared with wild-type and *kqt-2* mutants (Fig. 4A). By contrast, *kqt-2* mutants cultivated on 6.0-cm-diameter plates showed significantly increased cold acclimation compared with wild-type animals cultivated on 6.0-cm-diameter plates (Fig. 4A). These results indicated that other environmental factors in addition to cultivating temperature affect the cold acclimation phenotype of *kqt-2* mutants. Cold tolerance assays and Ca^{2+} imaging of *kqt-2* mutants indicate that ADL sensory neurons regulate cold acclimation (Fig. 2, A, E, and F). Previous studies report that oxygen signaling from URX sensory neurons indirectly modulates neuronal activation in ADL neurons evoked by the pheromone ascaroside through electrical synapses from RMG interneurons (*30*). We hypothesized that a difference of oxygen concentration between 3.5- and 6.0-cm-diameter plates affected the abnormal cold acclimation phenotype of *kqt-2* mutants. Previous studies reported that oxygen concentrations on the surface of agar plates are severely affected by the presence of a bacterial lawn (*29*). To examine whether oxygen concentrations differ between the two sizes of agar plates used for our cold acclimation assays, we optically measured oxygen concentration on the surface of assay plates (3.5 and 6.0 cm diameter) seeded with bacterial lawns and worms and sealed with parafilm. Optical oxygen concentration measurements were made from 24 to 64 hours after egg laying at the beginning of our protocol. We found that oxygen concentrations in the bacterial lawn of 3.5-cm-diameter plates were lower compared with that in 6.0-cm-diameter plates, stabilizing to values of ~15% O_2 for 6.0-cm-diameter plates and ~10% O_2 for 3.5-cm-diameter plates from 52 to 64 hours after egg laying (Fig. 4B).

To examine whether oxygen signaling affects cold acclimation regulated by ADL neurons, we used a *gcy-35* mutation, defective in the oxygen receptor expressed in URX oxygen sensory neurons (*37*). We found that *gcy-35* mutant animals showed an abnormal decrease in cold acclimation, which was opposite the phenotype observed with *kqt-2* mutants (Fig. 4C). The supranormal cold acclimation of the *kqt-2* mutant was suppressed by *gcy-35* mutation in *gcy-35;kqt-2* double mutants (Fig. 4C). Ca^{2+} imaging demonstrated that the abnormal dampening of the thermosensitive Ca^{2+} response in ADL neurons observed in *kqt-2* mutants was restored to wild-type levels by *gcy-35* mutation (Fig. 4, D and E). These results indicate that the oxygen receptor GCY-35 modulates both thermosensory function in ADL neurons and organismal cold acclimation.

We also found that abnormally enhanced cold acclimation of the *kqt-2* mutant was recovered to normal levels after cultivation with a lower O_2 concentration (10 or 5%) in the incubator (Fig. 4F). These results are consistent with a mechanism whereby supranormal cold acclimation observed in *kqt-2* mutants is enhanced by higher O_2 concentration through an indirect negative modulation of thermosensation in ADL neurons via active O_2 signaling from URX and RMG.

DISCUSSION

Elucidation of temperature acclimation mechanisms is important for understanding the biological mechanisms of long-term temperature responses in living organisms. The results of this study show that oxygen acts as a modulator of temperature sensation in a small neural circuit critical for cold acclimation in *C. elegans*.

Physiological and genetic analyses show that thermosensitive neuronal activity in ADL sensory neurons regulates cold acclimation. Our results indicate that KQT-type potassium channel subunits, KQT-2 and KQT-3, in ADL sensory neurons regulate cold acclimation, with KQT-2 acting as a negative regulator of functional activity, as measured by thermosensitive Ca^{2+} influx in ADL neurons (Fig. 4G). As previously reported, *kqt-2* gene expression is increased by a temperature shift from 23° to 17°C for 4 hours (*35*). On the basis of this result, wild-type animals treated to a 25°C→15°C (3 hours) conditioning step used in our cold acclimation assay likely induces increased *kqt-2* gene expression relative to unconditioned control animals cultivated at 25°C. KCNQ-type potassium channel subunits, KCNQ2 and KCNQ3, coassemble to form the native functional channels that underlie M-currents (*36*). Similar to KCNQ channel subunits, KQT-2 subunits expressed at lower temperatures (15° to 17°C) after cultivation at 25°C (*35*) possibly coassemble with KQT-3 subunits to form inactive KQT-2/KQT-3 heteromeric channels, leading to a reduction of functional potassium channel activity.

The KQT-2 subunit increases neuronal excitability in ADL neurons by acting as a negative regulator of KQT-3 channel function. By contrast, the OCR-1 TRP channel subunit decreases neuronal excitability of ADL neurons by acting as a negative regulator of OCR-2/OSM-9 TRP channels (Fig. 4G). Thus, these regulatory subunits appear to play a similar inhibitory role in two different ion channels, TRP and KQT, responsible for depolarizing and hyperpolarizing ADL sensory neurons, respectively.

The abnormally enhanced cold acclimation phenotype of the *kqt-2* mutant is influenced by cultivation oxygen concentration. Oxygen signaling from URX oxygen-sensing neurons modulates ADL excitability for sensing the nematode pheromone, ascaroside, through chemical and electrical synaptic connections via RMG interneurons (*30*). Thermally induced Ca^{2+} influx in ADL neurons was blunted in *kqt-2* mutants, and *kqt-2* mutants exhibited supranormal cold acclimation (Fig. 4H, middle panel). By contrast, mutation in *gcy-35*, which encodes the oxygen receptor in URX, strongly suppressed the blunted thermoexcitability of ADL neurons and restored cold acclimation in *kqt-2;gcy-35* double mutants to wild-type levels (Fig. 4H, right panel). Our study suggests that the environmental oxygen sensed by URX sensory neurons and the temperature sensed by ADL neurons may integrate in ADL to determine cold acclimation in a simple neural circuit.

Wild-type worms cultivated at 15°C and *kqt-2* mutants cultivated at 25°C both exhibited increased cold acclimation and decreased thermal responsiveness in ADL neurons compared with controls. This indicates that decreased neuronal activity in ADL neurons may directly induce enhanced cold acclimation. However, *kqt-3* or *ocr-1* mutants, which both increase ADL thermal responsiveness, exhibit increased and normal cold acclimation, respectively. In addition, *gcy-35* mutants, which show decreased cold acclimation compared with wild-type, nonetheless exhibit normal ADL thermal responsiveness. Therefore, although cold acclimation is regulated by ADL activity, additional neuronal mechanisms likely contribute to this phenotype and remain to be identified.

Our previous studies reported that cold tolerance is regulated by ASJ thermosensory neurons, sperm, intestine, and muscles (*7, 15–17*). ASJ neurons secrete insulin to intestinal cells to control cold tolerance (*7*), and sperm affects the activity of ASJ temperature-sensing neurons in cold tolerance (*16*). Our present study also indicates that sperm affects ADL temperature-sensing neurons because the *kqt-2* mutation suppresses the abnormal cold acclimation of *gsp-4* mutants lacking sperm (fig. S8, A and B). Together, these results indicate that interactions between these tissues could govern cold acclimation.

Mutation in the oxygen receptor gene, *gcy-35* in URX, decreased cold acclimation and suppressed the enhanced cold acclimation and decreased thermal responsiveness of ADL neurons in *kqt-2* mutants. In addition, *kqt-2* mutants showed decreased cold acclimation when cultivated at 10% O_2 compared with 20% O_2; however, *gcy-35* mutants similarly cultivated at 10% O_2 failed to exhibit decreased cold acclimation compared with cultivation at 20% O_2 (Fig. 4F and fig. S7B). These results indicate that oxygen signaling from URX neurons modulates ADL activity and affects cold acclimation. However, *gcy-35* mutants cultivated in 5% O_2 and *gcy-35;kqt-2* mutants cultivated in 5 or 10% O_2 both showed decreased cold acclimation compared with 20% O_2–cultivated controls, indicating that other oxygen receptor protein(s) besides GCY-35 may affect cold acclimation (fig. S7, A to C). *gcy-35* mutants showed normal ADL thermal responsiveness, although the *gcy-35* mutation suppressed the increased ADL thermal responsiveness of *kqt-2* mutants. ADL activity in *gcy-35* mutants was normal, possibly because other oxygen receptors provide redundant oxygen signaling to ADL neurons. However, the *kqt-2* mutation alone decreases thermal responsiveness, whereas the *gcy-35* mutant restores thermal responsiveness to wild-type levels in the *gcy-35;kqt-2* double mutant. This indicates a preferential role for O_2 signaling via GCY-35 if additional oxygen-sensing mechanisms are involved in cold acclimation. Together, these findings indicate that the cold acclimation status of individual animals may be controlled by complex neural circuitry and tissue networks involving known cold tolerance–related cells, such as ASJ neurons, intestine, sperm, and muscle, as well as other unidentified cells.

This and previous studies reveal that ADL neurons play various thermosensory and chemosensory roles and integrate chemosensory and thermosensory information with signaling from O_2-sensing neurons (*17*, *30, 33*). The *kqt-2* mutant showed not only abnormal cold acclimation but also abnormal chemosensory avoidance behavior. KQT-2 modulates ADL responsiveness to other environmental factors in addition to temperature and is possibly involved in signal transduction in response to environmental factors.

Many fundamental molecular and physiological aspects of neural systems are evolutionally conserved from *C. elegans* to mammals. The regulatory mechanisms revealed by these studies in *C. elegans* may be conserved as long-term adaptive strategies in higher organisms to similarly control neuronal excitability in response to sustained shifts in external or internal environmental stresses.

MATERIALS AND METHODS

Strains

We used the following *C. elegans* strains: N2 Bristol England; RB1415 *catp-3(ok1612)*; VC693 *cgt-1(ok1045)*; RB2095 *clec-67(ok2770)*; RB1262 *cpr-1(ok1344)*; FX2418 *dhs-4(tm2418)*; RB1772 *dmd-7(ok2776)*; FX2468 *F58E6.7(tm2468)*; NL795 *gpa-7(pk610)*; RB1373 *gpdh-1(ok1558)*; RB883 *kqt-2(ok732)*; CZ1758 *max-1(ju142)*; FX1770 *mtl-1(tm1770)*; FX830 *pgp-9(tm830)*; RB908 *pmp-1(ok773)*, *T28C12.4(tm1013)*, *kqt-2(tm642)*; CX0010 *osm-9(ky10)*; FK127 *tax-4(p678)*; ZK64 *kqt-3(aw1)*; CX4533 *ocr-1(ok132)*; CX4544 *ocr-2(ak47)*; CX6448 *gcy-35(ok769)*; CX4652 *ocr-2(ak47) osm-9(ky10)*; FX05415 *gsp-4(tm5415)*.

Cold acclimation assay

Cold acclimation was assayed essentially according to previous reports (*38*). *C. elegans* were cultured under well-fed conditions on 2% (w/v) agar nematode growth medium (NGM) plates containing *Escherichia coli* OP50 in 3.5- or 6.0-cm-diameter plastic dishes. Single or several well-fed adults (P_0) were placed at the first temperature and incubated for 15 to 20 or 2 to 4 hours, respectively, until they had laid ~100 eggs. P_0 adults were then removed to synchronize the growth of the progeny. Progenies were incubated from egg to adulthood at the initial (cultivation) temperature. At 15°C cultivation temperature, progenies were cultured for 132 to 150 hours; at 25°C cultivation temperature, progenies were cultured for 52 to 67 hours. When animals grew to adults, assay plates were transferred to a second (conditioning) temperature for 0, 3, 5, or 8 hours. After incubation at the second temperature, plates were immediately chilled on ice for 20 min and then transferred to a 2°C refrigerator (CRB-41A, Hitachi, Japan) for 48 hours. After 48 hours at 2°C, assay plates were transferred to and incubated at 15°C for 1 day. The numbers of live and dead worms were then scored. Cold acclimation assays at specified oxygen concentrations were performed using an airtight bag kit containing oxygen meter and oxygen adsorbent [BIONIX-3 (nB-3), SUGIYAMA-GEN, Japan], which allowed us to control oxygen concentration in the temperature shift protocol, 25°C→15°C (3 hours)→2°C. Each cold acclimation assay was performed with more than three plates. Alive and dead animals were counted on plates with more than 30 worms. The cold acclimation assays were performed on at least three independent days to obtain stable data.

Confocal microscopy

Worms were anesthetized and mounted in 10-μl drops of 100 mM NaN_3 on thin 2% agar pads formed on glass microscope slides. Immobilized worms were coverslipped for confocal microscopy. Fluorescent images were acquired with a confocal laser microscope (FV1000-IX81 with a GaAsP photomultiplier tube, Olympus) using FV10-ASW software (Olympus). We observed wild-type animals expressing plasmid constructs containing 5′ *kqt-2* promoter sequence (9.0 kb) with the *kqt-2* genomic sequence encompassing exons 1 to 12, with GFP fused in frame to the C terminus in exon 12.

DiI staining of amphid (ADL, ASH, ASI, ASJ, ASK, and AWB) and phasmid (PHA and PHB) neurons

DiI staining was performed following the protocol in Anatomical Methods in WORMATLAS (www.wormatlas.org/EMmethods/DiIDiO.htm). DiI stock solution (5 mg/ml) was stored at −20°C in a foil-wrapped tube. Staining solution was made by diluting 0.7 μl of DiI stock solution in 2.0 ml of M9. Staining solution (150 μl) was placed in a 200-ml tube, into which worms were transferred. Worms were incubated in DiI staining solution for 1 hour at room temperature. A pipette was used to transfer stained worms to a fresh plate with a bacterial lawn. Worms were allowed to destain for about an hour by crawling on the bacterial lawn. Destained worms were mounted on agar pads with sodium azide and visualized for fluorescence using the appropriate filter sets.

Germline transformation

Germline transformations were performed with coinjection mixes consisting of experimental plasmid DNAs at various concentrations (5.0 to 50 ng/μl) and pAK62 *AIYp::GFP*, pKDK66 *ges-1p::NLS::GFP*, or pRF4 *rol-6gf* as transgenic markers at 30 to 50 ng/μl.

Behavioral analysis

Avoidance behavior was assayed essentially as described by a previous report (*39*). *C. elegans* were cultured under well-fed conditions on 2% (w/v) agar NGM plates containing *E. coli* OP50 in 6.0-cm-diameter plastic dishes. Two or three well-fed adults (P_0) were placed and incubated for about 20 hours until they had laid ~200 eggs. P_0 adults were then removed to synchronize the growth of the progeny. Progenies were incubated from egg to adulthood at 20°C. The assay plates, 9-cm-diameter medium plates [2% agar, 1 mM $MgSO_4$, 1 mM $CaCl_2$, and 25 mM potassium phosphate (pH 6.0)], were divided into 12 sectors (#1 to 12) of equal width. The adult animals were collected with NG buffer from the cultivation plates, put into a 1.5-ml tube, and washed twice with NG buffer. Washed animals were put on the center of a 9-cm-diameter medium plate. After the buffer was removed, 1-octanol was put in two spots on the third line from the left. The assay plates were left to stand for 12 min. To stop the movement of animals after 12 min, animals were exposed to $CHCl_3$. Assays were repeated for 4 days. The numbers of animals in each fraction were counted, and an avoidance index was calculated using the formula: Avoidance index = ΣWiNi/N [Wi: −2.5(#1), −2.0(#2), −1.5(#3), −1.0(#4), −0.5(#5), −0.25(#6), +0.25(#7), +0.5(#8), +1.0(#9), +1.5(#10), +2.0(#11), +2.5(#12); Ni: the number of animals in each sector; N: the total number of animals in all sectors of the plate]. The animals that did not move from the center of the plate were not scored.

In vivo calcium imaging

In vivo calcium imaging of ADL sensory neurons was performed essentially as described previously (*7, 40*). Worms expressing yellow cameleon 3.60 (YC3.60) driven by the *sre-1p* promoter [*sre-1p::yc3.60* (pTOM63)] were used for in vivo calcium imaging of ADL neurons. Animals were cultured under well-fed conditions on 2% (w/v) agar NGM plates containing *E. coli* OP50 in 6.0-cm-diameter plastic dishes. Two or three well-fed adult(s) (P_0) were placed onto NGM plates at 25° or 15°C, and their progenies were incubated at 25° or 15°C from egg to adulthood for 3 or 6 days, respectively. Adult animals were glued onto a 2% (w/v) agar pad on a glass slide and immersed in M9 buffer under a glass coverslip. Sample preparation was completed within 3 min. Samples were then placed onto an indium tin oxide glass-based thermocontroller (Tokai Hit Co. Ltd., Fujinomiya, Japan) mounted on the stage of an Olympus IX81 microscope (Olympus Corporation, Tokyo, Japan) and equilibrated at the initial imaging temperature for a few minutes. Fluorescence was observed using a Dual-View (Molecular Devices, USA) optical system. YC3.60 donor and acceptor fluorescent signals were captured simultaneously using an electron multiplying charge-coupled device camera (Evolve 512, Photometrics, USA). Images were taken with 30-ms exposure times and 1 × 1 binning. Temperature on the agar pad was monitored using a thermometer system (MATS-5500RA-KY, Tokai Hit). For each imaging experiment, fluorescence intensities were acquired and processed using MetaMorph (Molecular Devices) image analysis software. Relative changes in intracellular calcium concentrations were measured as changes in the acceptor/donor fluorescence ratio of YC3.60. Band-pass filters for all YC3.60 experiments were as described in a previous report (*40*).

Measurement of oxygen concentration

We measured oxygen concentration optically using the PreSens OXY-1 SMA system (PreSens Precision Sensing GmbH, Germany), which allowed us to measure oxygen concentration through the cover of airtight NGM plates. We placed "oxygen sensor spots" (SP-PSt3-NAU-D5-YOP, PreSens Precision Sensing GmbH, Germany) in the bacterial lawn of individual agar plates. Well-fed adults (P_0) were placed on 3.5- or 6.0-cm-diameter NGM plates with oxygen sensor spots and incubated for 2 to 3 hours until about 60 to 100 eggs were laid, after which the adult worms were removed. After egg laying, plates were tightly sealed with parafilm and cultivated at 25°C. Oxygen concentration was noninvasively monitored by shining excitation light onto the oxygen sensor spots through an optical fiber from 24 to 64 hours after egg laying. OXY-1 SMA oxygen concentrations were continuously recorded once a second. Oxygen concentrations were calculated as the running average of measurements every 10 s.

Statistical analysis

The cold acclimation tests were performed on more than eight plates on at least three independent days. All error bars in the figures indicate the SEM. Assuming that the distributions of all data follow normal distribution, all statistical analyses were performed using parametric tests, the Tukey-Kramer method, Dunnett's test, or the unpaired *t* test (Welch). Multiple comparisons were performed using one-way analysis of variance (ANOVA) with comparison tested using the Tukey-Kramer method and Dunnett's test. Dunnett's test was performed to compare the leftmost groups of the bar graphs with other groups. Comparisons between two groups were performed using the unpaired *t* test (Welch). $*P < 0.05$, $**P < 0.01$. We have performed two-way ANOVA in Fig. 2L (see "Supplementary raw data file"). The tests were performed using Mac statistical analysis version 2 (Esumi, Japan).

SUPPLEMENTARY MATERIALS

Supplementary material for this article is available at http://advances.sciencemag.org/cgi/content/full/5/2/eaav3631/DC1
Supplementary Results and Discussion
Supplementary Methods
Fig. S1. Cold acclimation assays of selected mutant animals defective in genes identified by previous DNA microarray analysis.
Fig. S2. Localization analysis of KQT-2.
Fig. S3. Lipid composition of wild-type and *kqt-2(ok732)*.
Fig. S4. Behavioral assays of *kqt-2(ok732)*.
Fig. S5. Cold acclimation assays of *kqt-1(ok413)*.
Fig. S6. Ca^{2+} imaging of ADL neurons in mutants defective in TRP channels expressed in ADL neurons.
Fig. S7. Cold acclimation of animals cultivated with O_2 concentrations of 20, 10, and 5%.
Fig. S8. Cold acclimation assays with mutants defective in GSP-4, a sperm-specific protein phosphatase (PP1).
Supplementary raw data file

REFERENCES AND NOTES

1. A. Dhaka, V. Viswanath, A. Patapoutian, Trp ion channels and temperature sensation. *Annu. Rev. Neurosci.* **29**, 135–161 (2006).
2. W. L. Shen, Y. Kwon, A. A. Adegbola, J. Luo, A. Chess, C. Montell, Function of rhodopsin in temperature discrimination in *Drosophila*. *Science* **331**, 1333–1336 (2011).
3. A. Takeishi, Y. V. Yu, V. M. Hapiak, H. W. Bell, T. O'Leary, P. Sengupta, Receptor-type guanylyl cyclases confer thermosensory responses in *C. elegans*. *Neuron* **90**, 235–244 (2016).
4. N. Fielenbach, A. Antebi, *C. elegans* dauer formation and the molecular basis of plasticity. *Genes Dev.* **22**, 2149–2165 (2008).
5. A. Kuhara, M. Okumura, T. Kimata, Y. Tanizawa, R. Takano, K. D. Kimura, H. Inada, K. Matsumoto, I. Mori, Temperature sensing by an olfactory neuron in a circuit controlling behavior of *C. elegans*. *Science* **320**, 803–807 (2008).
6. I. Mori, Y. Ohshima, Neural regulation of thermotaxis in *Caenorhabditis elegans*. *Nature* **376**, 344–348 (1995).
7. A. Ohta, T. Ujisawa, S. Sonoda, A. Kuhara, Light and pheromone-sensing neurons regulates cold habituation through insulin signalling in *Caenorhabditis elegans*. *Nat. Commun.* **5**, 4412 (2014).
8. D. A. Glauser, W. C. Chen, R. Agin, B. L. MacInnis, A. B. Hellman, P. A. Garrity, M. W. Tan, M. B. Goodman, Heat avoidance is regulated by transient receptor potential (TRP) channels and a neuropeptide signaling pathway in *Caenorhabditis elegans*. *Genetics* **188**, 91–103 (2011).
9. N. Wittenburg, R. Baumeister, Thermal avoidance in *Caenorhabditis elegans*: An approach to the study of nociception. *Proc. Natl. Acad. Sci. U.S.A.* **96**, 10477–10482 (1999).
10. L. C. Schild, D. A. Glauser, Dynamic switching between escape and avoidance regimes reduces *Caenorhabditis elegans* exposure to noxious heat. *Nat. Commun.* **4**, 2198 (2013).
11. R. Xiao, B. Zhang, Y. Dong, J. Gong, T. Xu, J. Liu, X. Z. S. Xu, A genetic program promotes C. elegans longevity at cold temperatures via a thermosensitive TRP channel. *Cell* **152**, 806–817 (2013).
12. F. R. Savory, S. M. Sait, I. A. Hope, DAF-16 and Δ^9 desaturase genes promote cold tolerance in long-lived *Caenorhabditis elegans age-1* mutants. *PLOS ONE* **6**, e24550 (2011).
13. P. Murray, S. A. L. Hayward, G. G. Govan, A. Y. Gracey, A. R. Cossins, An explicit test of the phospholipid saturation hypothesis of acquired cold tolerance in *Caenorhabditis elegans*. *Proc. Natl. Acad. Sci. U.S.A.* **104**, 5489–5494 (2007).
14. A. Ohta, A. Kuhara, Molecular mechanism for trimetric G protein-coupled thermosensation and synaptic regulation in the temperature response circuit of *Caenorhabditis elegans*. *Neurosci. Res.* **76**, 119–124 (2013).
15. T. Ujisawa, A. Ohta, M. Uda-Yagi, A. Kuhara, Diverse regulation of temperature sensation by trimeric G-protein signaling in *Caenorhabditis elegans*. *PLOS ONE* **11**, e0165518 (2016).
16. S. Sonoda, A. Ohta, A. Maruo, T. Ujisawa, A. Kuhara, Sperm affects head sensory neuron in temperature tolerance of *Caenorhabditis elegans*. *Cell Rep.* **16**, 56–65 (2016).
17. T. Ujisawa, A. Ohta, T. Ii, Y. Minakuchi, A. Toyoda, M. Ii, A. Kuhara, Endoribonuclease ENDU-2 regulates multiple traits including cold tolerance via cell autonomous and nonautonomous controls in*Caenorhabditis elegans*. *Proc. Natl. Acad. Sci. U.S.A.* **115**, 8823–8828 (2018).
18. M. Okahata, A. Ohta, H. Mizutani, Y. Minakuchi, A. Toyoda, A. Kuhara, Natural variations of cold tolerance and temperature acclimation in *Caenorhabditis elegans*. *J. Comp. Physiol. B* **186**, 985–998 (2016).
19. T. J. Jentsch, Neuronal KCNQ potassium channels: Physiology and role in disease. *Nat. Rev. Neurosci.* **1**, 21–30 (2000).
20. C. Charlier, N. A. Singh, S. G. Ryan, T. B. Lewis, B. E. Reus, R. J. Leach, M. Leppert, A pore mutation in a novel KQT-like potassium channel gene in an idiopathic epilepsy family. *Nat. Genet.* **18**, 53–55 (1998).
21. N. A. Singh, P. Westenskow, C. Charlier, C. Pappas, J. Leslie, J. Dillon, V. E. Anderson, M. C. Sanguinetti, M. F. Leppert; BFNC Physician Consortium, *KCNQ2* and *KCNQ3* potassium channel genes in benign familial neonatal convulsions: Expansion of the functional and mutation spectrum. *Brain* **126**, 2726–2737 (2003).
22. C. Biervert, B. C. Schroeder, C. Kubisch, S. F. Berkovic, P. Propping, T. J. Jentsch, O. K. Steinlein, A potassium channel mutation in neonatal human epilepsy. *Science* **279**, 403–406 (1998).
23. N. Neyroud, F. Tesson, I. Denjoy, M. Leibovici, C. Donger, J. Barhanin, S. Fauré, F. Gary, P. Coumel, C. Petit, K. Schwartz, P. Guicheney, A novel mutation in the potassium channel gene KVLQT1 causes the Jervell and Lange-Nielsen cardioauditory syndrome. *Nat. Genet.* **15**, 186–189 (1997).
24. Q. Wang, M. E. Curran, I. Splawski, T. C. Burn, J. M. Millholland, T. J. VanRaay, J. Shen, K. W. Timothy, G. M. Vincent, T. de Jager, P. J. Schwartz, J. A. Towbin, A. J. Moss, D. L. Atkinson, G. M. Landes, T. D. Connors, M. T. Keating, Positional cloning of a novel potassium channel gene: *KVLQT1* mutations cause cardiac arrhythmias. *Nat. Genet.* **12**, 17–23 (1996).
25. A. D. Wei, A. Butler, L. Salkoff, KCNQ-like potassium channels in *Caenorhabditis elegans*. Conserved properties and modulation. *J. Biol. Chem.* **280**, 21337–21345 (2005).
26. K. Nehrke, J. Denton, W. Mowrey, Intestinal Ca^{2+} wave dynamics in freely moving *C. elegans* coordinate execution of a rhythmic motor program. *Am. J. Physiol. Cell Physiol.* **294**, C333–C344 (2008).
27. A. A. Abd-Elsayed, R. Ikeda, Z. Jia, J. Ling, X. Zuo, M. Li, J. G. Gu, KCNQ channels in nociceptive cold-sensing trigeminal ganglion neurons as therapeutic targets for treating orofacial cold hyperalgesia. *Mol. Pain* **11**, 45 (2015).
28. B. H. Cheung, F. Arellano-Carbajal, I. Rybicki, M. de Bono, Soluble guanylate cyclases act in neurons exposed to the body fluid to promote C. elegans aggregation behavior. *Curr. Biol.* **14**, 1105–1111 (2004).
29. J. M. Gray, D. S. Karow, H. Lu, A. J. Chang, J. S. Chang, R. E. Ellis, M. A. Marletta, C. I. Bargmann, Oxygen sensation and social feeding mediated by a *C. elegans* guanylate cyclase homologue. *Nature* **430**, 317–322 (2004).
30. L. A. Fenk, M. de Bono, Memory of recent oxygen experience switches pheromone valence in *Caenorhabditis elegans*. *Proc. Natl. Acad. Sci. U.S.A.* **114**, 4195–4200 (2017).
31. C. Montell, The TRP superfamily of cation channels. *Sci. STKE* 2005, re3 (2005).
32. H. A. Colbert, T. L. Smith, C. I. Bargmann, OSM-9, a novel protein with structural similarity to channels, is required for olfaction, mechanosensation, and olfactory adaptation in *Caenorhabditis elegans*. *J. Neurosci.* **17**, 8259–8269 (1997).
33. M. de Bono, D. M. Tobin, M. W. Davis, L. Avery, C. I. Bargmann, Social feeding in *Caenorhabditis elegans* is induced by neurons that detect aversive stimuli. *Nature* **419**, 899–903 (2002).
34. A. M. Jose, I. A. Bany, D. L. Chase, M. R. Koelle, A specific subset of transient receptor potential vanilloid-type channel subunits in *Caenorhabditis elegans* endocrine cells function as mixed heteromers to promote neurotransmitter release. *Genetics* **175**, 93–105 (2007).
35. T. Sugi, Y. Nishida, I. Mori, Regulation of behavioral plasticity by systemic temperature signaling in *Caenorhabditis elegans*. *Nat. Neurosci.* **14**, 984–992 (2011).
36. H.-S. Wang, Z. Pan, W. Shi, B. S. Brown, R. S. Wymore, I. S. Cohen, J. E. Dixon, D. McKinnon, KCNQ2 and KCNQ3 potassium channel subunits: Molecular correlates of the M-channel. *Science* **282**, 1890–1893 (1998).
37. A. Persson, E. Gross, P. Laurent, K. E. Busch, H. Bretes, M. de Bono, Natural variation in a neural globin tunes oxygen sensing in wild *Caenorhabditis elegans*. *Nature* **458**, 1030–1033 (2009).
38. T. Ujisawa, A. Ohta, M. Okahata, S. Sonoda, A. Kuhara, Cold tolerance assay for studying cultivation-temperature-dependent cold habituation in *C. elegans*. *Protoc. Exch.* (2014).
39. E. R. Troemel, B. E. Kimmel, C. I. Bargmann, Reprogramming chemotaxis responses: Sensory neurons define olfactory preferences in C. elegans. *Cell* **91**, 161–169 (1997).
40. A. Kuhara, N. Ohnishi, T. Shimowada, I. Mori, Neural coding in a single sensory neuron controlling opposite seeking behaviours in *Caenorhabditis elegans*. *Nat. Commun.* **2**, 355 (2011).

Acknowledgments: We thank C. I. Bargmann for sharing strains; the National BioResource Project (Japan) and the Caenorhabditis Genetic Center for strains; T. Miura, T. Ujisawa, and other members of Kuhara laboratory for supporting experiments and discussion; K. Kanai for supporting experimental systems; and anonymous reviewers for invaluable comments on the manuscript. We thank J. Allen from Edanz Group (www.edanzediting.com/ac) for editing a draft of this manuscript. **Funding:** A.K. was supported by the Takeda Science Foundation, the Daiichi Sankyo Foundation of Life Science, the Naito Foundation, the Sumitomo Foundation, the Hirao Taro Foundation of KONAN GAKUEN for Academic Research, AMED Mechano Biology (18gm5810024h0002), JSPS KAKENHI (15K21744, 17K19410, and 18H02484), and KAKENHI (15H05928 and 16H06279) from MEXT Japan. A.O. was supported by the Daiichi Sankyo Foundation of Life Science, the Takeda Science Foundation, the Novartis Foundation, the Ono Medical Research Foundation, the Naito Foundation, and JSPS KAKENHI (16J00123 and 18K06344). M.O. was supported by JSPS KAKENHI (17J00642). A.D.W. was supported by Seattle Children's Research Institute, and some reagents used were created with funding from

the NSF (USA; IBN-0117341; A.D.W.). **Author contributions:** M.O., A.O., and A.K. performed the experiments. All authors designed the experiments, interpreted the results, and wrote the final report. **Competing interests:** The authors declare that they have no competing interests. **Data and materials availability:** All data needed to evaluate the conclusions in the paper are present in the paper and/or the Supplementary Materials, and requests for materials should be addressed to A.O. and A.K. Further information regarding data, figures, and other research findings in this study may be requested from the corresponding authors.

Submitted 10 September 2018
Accepted 21 December 2018
Published 6 February 2019
10.1126/sciadv.aav3631

Citation: M. Okahata, A. D. Wei, A. Ohta, A. Kuhara, Cold acclimation via the KQT-2 potassium channel is modulated by oxygen in *Caenorhabditis elegans*. *Sci. Adv.* **5**, eaav3631 (2019).